



Contents lists available at ScienceDirect

## Journal of the Mechanics and Physics of Solids

journal homepage: [www.elsevier.com/locate/jmps](http://www.elsevier.com/locate/jmps)

## Frictional energy dissipation in materials containing cracks

Yong Hoon Jang<sup>a,\*</sup>, J.R. Barber<sup>b,c</sup><sup>a</sup> School of Mechanical Engineering, Yonsei University, Shincheon-Dong 134, Seodaemun-Gu, Seoul 120-749, Republic of Korea<sup>b</sup> Department of Mechanical Engineering, University of Michigan, Ann Arbor, MI 48109-2125, USA<sup>c</sup> Department of Civil and Environmental Engineering, University of Michigan, Ann Arbor, MI 48109-2125, USA

## ARTICLE INFO

## Article history:

Received 24 February 2010

Received in revised form

20 August 2010

Accepted 19 December 2010

Available online 23 December 2010

## Keywords:

Fracture mechanics

Contact mechanics

Crack mechanics

Friction

Damage mechanics

## ABSTRACT

Kachanov's simplified model of microcrack interaction is applied to an investigation of the behaviour of a cracked body under predominantly compressive periodic loading, so that the cracks experience periods of closure and slip, with frictional dissipation. The model is shown to be equivalent to a discrete elastic frictional system with each crack representing one node. Theorems and algorithms from such systems are applied to determine the conditions under which the system shakes down to a state with no slip and hence no energy dissipation in friction. For conditions not too far beyond the shakedown state, the dissipation is significantly affected by the initial conditions, but with larger oscillating loads, it becomes a unique and increasing function of load amplitude. The effect of crack interaction is assessed by comparison with an uncoupled model, for which the dissipation is obtained as a summation of closed form expressions over the crack population. For small numbers of cracks, the results are significantly dependent on the randomly chosen crack locations and sizes, but with larger populations, a statistically significant decrease in dissipation is observed with increasing interaction terms.

© 2010 Elsevier Ltd. All rights reserved.

## 1. Introduction

The behaviour of materials is heavily influenced by the presence of imperfections such as grain boundaries, dislocations, inclusions and cracks, and numerous authors (e.g. *Gambarotta and Lagomarsino, 1993*; *Shao and Rudnicki, 2000*) have investigated the effects of such micromechanical features on the overall constitutive behaviour and on failure criteria. If the defects are widely separated, the effect of each can be investigated under a given external loading and the cumulative effects then summed by superposition, using an appropriate statistical description of the density of defects. However, in most cases this is an unrealistic idealization and interaction between neighbouring defects needs to be included. Various authors have assessed the significance of such interaction in particular cases, such as a periodic array of cracks (*Fleck, 1991*), or a dislocation near an elastic inclusion (*Gavazza and Barnett, 1974*).

For moderate crack densities, the interaction effect can be approximated by the first order term, which is equivalent to the assumption that the influence of deformation at one crack on the stress field in the vicinity of another crack can be approximated as being locally spatially uniform. *Kachanov (1987)* has defined a simple model based on this approximation and both his results and those of other researchers (*Basista and Gross, 2000*; *Li et al., 2003*; *Gorbatikh et al., 2007*) demonstrate that the predictions are quite accurate except in cases where the cracks are extremely close together.

In this paper, we shall use a first order model to examine the response of a two-dimensional body with a random distribution of  $N$  plane cracks to low frequency periodic loading. We shall pay particular attention to the case where the

\* Corresponding author.

E-mail address: [jyh@yonsei.ac.kr](mailto:jyh@yonsei.ac.kr) (Y.H. Jang).

externally applied stress field is predominantly compressive, so that many or all of the cracks experience periods of contact and possibly sliding friction. This leads to the dissipation of energy in friction, which is a contributor to hysteretic damping in the material.

We shall show that under these assumptions, the system can be completely characterized by a discrete system with 2N degrees of freedom, whose behaviour mimics that of an N-node discrete contact problem with frictional boundary conditions. Important results from such systems can therefore be carried over directly to the micromechanical problem.

## 2. Crack in an otherwise uniform stress field

Consider the case where a large plate containing a single plane crack of length  $2a_i$  is exposed to a time-varying far-field stress. There is no loss of generality in taking the crack to occupy the region  $-a_i < x_i < a_i$  on the line  $y_i=0$ , in which case the behaviour of the crack depends only on the time evolution of the far-field stress components  $\sigma_{yy}^{(i)}, \sigma_{yx}^{(i)}$  defined in these local coordinates.

If the crack is closed, we anticipate that shear and normal tractions will be transmitted between the faces, which we denote by  $q_i(x_i), p_i(x_i)$ , respectively. We adopt the sign convention that  $q_i, p_i$  act in the positive  $x_i, y_i$  directions, respectively on the surface of the half-plane  $y_i > 0$ , which implies that  $p_i$  is positive when compressive. Following the notation in Klarbring et al. (2007) and Ahn et al. (2008), we write the contact tractions in the form

$$q_i = q_i^w + \hat{q}_i, \quad p_i = p_i^w + \hat{p}_i, \quad (1)$$

where  $q_i^w, p_i^w$  are the ‘bilateral’ tractions, which would be obtained if the crack was assumed to be welded shut with zero relative displacement, and  $\hat{q}_i, \hat{p}_i$  define a perturbation associated with opening and slip displacements at the crack. The above sign conventions imply that the bilateral solution is defined by the uniform tractions

$$q_i^w = -\sigma_{yx}^{(i)}, \quad p_i^w = -\sigma_{yy}^{(i)}. \quad (2)$$

If the applied normal stress component  $\sigma_{yy}^{(i)}$  is tensile, the crack will open completely and the shear and normal tractions  $q_i(x), p_i(x)$  acting on the crack face will be zero, implying that  $\hat{q}_i = -q_i^w$  and  $\hat{p}_i = -p_i^w$ . Alternatively, if  $\sigma_{yy}^{(i)}$  is compressive, the crack will close completely and the normal stress will be transmitted as a uniform contact pressure  $p_i(x) = -\sigma_{yy}^{(i)}$ , which is unaffected by the slip displacement, if any.

Slip will not occur as long as the magnitude of the shear traction  $|q_i(x)| < \mu p_i(x)$  and, since  $p_i(x)$  is uniform, the limiting slip condition will be reached simultaneously at all points on the crack surface. Thus, at any given time  $t$ , all points on the crack interface  $-a_i < x_i < a_i$  must be in the same state (separation, slip or stick), and the contact tractions  $q_i(x), p_i(x)$  must be independent of  $x_i$ .

From the above discussion, we deduce that the perturbation in the stress and displacement fields due to the presence of the crack is completely characterized by a uniform normal traction  $\hat{p}_i$  and/or a uniform shear traction  $\hat{q}_i$  acting on the crack faces. This is a classical problem whose solution can be obtained using complex potentials (England, 1971), or by placing an appropriate distribution of glide and climb dislocations along the crack line (Barber, 2010; Hills et al., 1996). The resulting perturbation is defined by the displacement field

$$2\mu(u_x + nu_y) = \kappa\chi - \zeta\bar{\chi} - \bar{\theta}, \quad (3)$$

where  $\zeta = x_i + iy_i$ , the overbar denotes the complex conjugate and the holomorphic functions

$$\chi(\zeta) = \frac{(\hat{p}_i - i\hat{q}_i)}{2} \left( \sqrt{\zeta^2 - a_i^2} - \zeta \right), \quad (4)$$

$$\theta(\zeta) = -\frac{(\hat{p}_i + i\hat{q}_i)a_i^2}{2\sqrt{\zeta^2 - a_i^2}} + i\hat{q}_i\zeta \left( \frac{\zeta}{\sqrt{\zeta^2 - a_i^2}} - 1 \right) \quad (5)$$

(Bower, 2010). In particular, the crack opening displacement  $w_i(x_i)$  and the relative shear displacement  $v_i(x_i)$  between the crack faces are given by

$$v_i(x_i) = \frac{\hat{q}_i(\kappa + 1)\sqrt{a_i^2 - x_i^2}}{2\mu}, \quad w_i(x_i) = \frac{\hat{p}_i(\kappa + 1)\sqrt{a_i^2 - x_i^2}}{2\mu}. \quad (6)$$

In (3), (6),  $\mu$  is the modulus of rigidity of the material and  $\kappa = (3-4\nu)$  for plane strain and  $(3-\nu)/(1-\nu)$  for plane stress, with  $\nu$  being Poisson’s ratio.

### 2.1. Reduction to a discrete system

The above results show that the crack behaves like a single-node discrete frictional system with two degrees of freedom (opening and sliding) characterized by the parameters  $\hat{p}_i, \hat{q}_i$ . This analogy can be made more direct by defining the average displacements

$$v_i = \frac{1}{2a_i} \int_{-a_i}^{a_i} v_i(x_i) dx_i, \quad w_i = \frac{1}{2a_i} \int_{-a_i}^{a_i} w_i(x_i) dx_i \quad (7)$$

and the forces

$$Q_i = \int_{-a_i}^{a_i} q(x_i)dx_i = 2q_i a_i, \quad P_i = \int_{-a_i}^{a_i} p_i(x_i)dx_i = 2p_i a_i, \quad (8)$$

which are the total reaction forces transmitted across the crack surfaces. Substituting (6) into (7) and performing the integrals, we then obtain

$$v_i = \frac{\pi(\kappa+1)\hat{q}_i a_i}{8\mu} = \frac{\pi(\kappa+1)\hat{Q}_i}{16\mu}, \quad w_i = \frac{\pi(\kappa+1)\hat{p}_i a_i}{8\mu} = \frac{\pi(\kappa+1)\hat{P}_i}{16\mu}. \quad (9)$$

We also note that during slip, work will be done against friction at the crack surfaces at a rate

$$\dot{W}_i = - \int_{-a_i}^{a_i} q_i \dot{v}_i(x_i)dx_i \quad (10)$$

and since the tangential displacement always has the semi-elliptic form (6), the velocity

$$\dot{v}_i(x_i) = \frac{4\dot{v}_i \sqrt{a_i^2 - x_i^2}}{\pi a_i} \quad (11)$$

giving

$$\dot{W}_i = -Q_i \dot{v}_i \quad (12)$$

from (10). This is of course precisely the dissipation rate that would be obtained at a single contact node in a discrete frictional contact problem. We also note that the complex potentials can be expressed in terms of the average displacements  $v_i, w_i$  as

$$\chi(\zeta) = \frac{4\mu(w_i - iv_i)}{\pi(\kappa+1)a_i} \left( \sqrt{\zeta^2 - a_i^2} - \zeta \right), \quad (13)$$

$$\theta(\zeta) = - \frac{4\mu(w_i + iv_i)a_i}{\pi(\kappa+1)\sqrt{\zeta^2 - a_i^2}} + \frac{8\mu v_i \zeta}{\pi(\kappa+1)a_i} \left( \frac{\zeta}{\sqrt{\zeta^2 - a_i^2}} - 1 \right). \quad (14)$$

### 2.2. Evolution of the system

The frictional behaviour of the crack can now be characterized mathematically by the classical discrete Coulomb friction law

$$w_i \geq 0, \quad P_i \geq 0, \quad (15)$$

$$w_i > 0 \Rightarrow P_i = Q_i = 0, \quad (16)$$

$$P_i > 0 \Rightarrow w_i = 0, \quad (17)$$

$$|Q_i| \leq fP_i, \quad (18)$$

$$|Q_i| < fP_i \Rightarrow \dot{v}_i = 0, \quad (19)$$

$$0 < |Q_i| = fP_i \Rightarrow \text{sgn}(\dot{v}_i) = -\text{sgn}(Q_i), \quad (20)$$

where

$$P_i = P_i^w + \hat{P}_i = P_i^w + \frac{16\mu w_i}{\pi(\kappa+1)}, \quad Q_i = Q_i^w + \hat{Q}_i = Q_i^w + \frac{16\mu v_i}{\pi(\kappa+1)} \quad (21)$$

from (9). Conditions (16), (19), (20) define the states of separation, stick and slip, respectively.

### 3. First-order crack interaction

Suppose now that there are  $N$  microcracks of length  $a_i$ ,  $i \in (1, N)$  and that the perturbation at crack  $i$  is described by the average displacements  $v_i, w_i$ , defined as in Eq. (7). If the crack distribution is sufficiently sparse, the above results can be used to determine the conditions at each crack and hence to make predictions about the conditions at failure, the average constitutive behaviour of the material and the hysteretic damping under prescribed cyclic loading. For example, the total frictional dissipation will be a summation of Eq. (12) over all the cracks.

However, the conditions that the cracks all act independently is too restrictive to apply to most practical microstructures. Even if the density of microcracks is relatively low, they are unlikely to be 'homogeneously' distributed, and some features of the behaviour of the system may be influenced by regions in which some cracks are sufficiently close for their stress fields to

interact. Following [Kachanov \(1987\)](#), we shall restrict attention to ‘first-order interaction’, meaning that each crack is sufficiently distant from its nearest neighbours for the stress perturbation due to those neighbours to be regarded as locally uniform. The above results can then still be applied, except that the perturbation terms  $\hat{P}_j, \hat{Q}_j$  in Eq. (21) will now contain contributions that are linearly proportional to the perturbations at the other cracks. We express this formally by generalizing (21) to read

$$Q_j = Q_j^w + \sum_{i=1}^N A_{ji} v_i + \sum_{i=1}^N B_{ji} w_i, \quad P_j = P_j^w + \sum_{i=1}^N B_{ij} v_i + \sum_{i=1}^N C_{ji} w_i \quad (22)$$

or

$$\begin{Bmatrix} Q_j \\ P_j \end{Bmatrix} = \begin{Bmatrix} Q_j^w \\ P_j^w \end{Bmatrix} + \begin{bmatrix} A_{ji} & B_{ji} \\ B_{ij} & C_{ji} \end{bmatrix} \begin{Bmatrix} v_i \\ w_i \end{Bmatrix}, \quad (23)$$

where  $\mathbf{A}, \mathbf{B}, \mathbf{C}$  are matrices of influence coefficients which remain to be determined. The combined matrix in (23) is the stiffness matrix for the discrete system and hence must be symmetric. This implies that the sub-matrices  $\mathbf{A}, \mathbf{C}$  are symmetric and explains why the transpose of  $\mathbf{B}$  appears in (22)<sub>2</sub>. However,  $\mathbf{B}$  itself is not necessarily symmetric. Kachanov refers to these coefficients as *transmission factors*, but his definitions are slightly different from ours because he works with average crack tractions instead of nodal forces.

### 3.1. Influence coefficients

A first approximation to the influence of displacements  $w_i, v_i$  at crack  $i$  on the loading of crack  $j$  can be defined in terms of the stress perturbation due to crack  $i$  at the *centre* of crack  $j$ . However, [Kachanov \(1987\)](#) has shown that this imposes quite severe restrictions on the sparseness of the crack distribution, whereas the method gives quite good approximations for relatively dense populations of cracks if instead we use the *average* tractions on the crack line  $j$  due to displacements at crack  $i$ . In the present terminology, this implies that the terms  $A_{ji} v_i + B_{ji} w_i$  and  $B_{ij} v_i + C_{ji} w_i$  should represent the shear and normal components, respectively, of the resultant force transmitted across the surface of crack  $j$  in the stress field defined by the perturbation at crack  $i$ .

In the complex variable formalism, the resultant force transmitted across any such line is given by

$$F_x + iF_y = -i(\psi_A - \psi_B) \quad (24)$$

([Barber, 2010](#), Section 19.5), where  $\psi_A, \psi_B$  are the values of the complex function

$$\psi = \chi + \zeta \bar{\chi} + \bar{\theta} \quad (25)$$

at the two points  $\zeta_A, \zeta_B$  defining the ends of the line and the force acts on the surface that lies to the left as we go from  $\zeta_B$  to  $\zeta_A$ . For the crack problem, the potentials  $\chi, \theta$  are given by (13), (14) and we obtain

$$\psi = \frac{8\mu}{\pi(\kappa+1)} (\psi^{(v)} v_i + \psi^{(w)} w_i), \quad (26)$$

where

$$\psi^{(v)} = \frac{i\bar{\zeta}}{a_i} - \frac{i}{2a_i} \sqrt{\zeta^2 - a_i^2} - \frac{i(2\bar{\zeta}^2 - \zeta\bar{\zeta} - a_i^2)}{2a_i \sqrt{\zeta^2 - a_i^2}}, \quad (27)$$

$$\psi^{(w)} = -\frac{\zeta}{a_i} + \frac{1}{2a_i} \sqrt{\zeta^2 - a_i^2} + \frac{(\zeta\bar{\zeta} - a_i^2)}{2a_i \sqrt{\zeta^2 - a_i^2}}. \quad (28)$$

Suppose that the centres of cracks  $ij$  are located at the points  $\zeta_i, \zeta_j$  in a global system of Cartesian coordinates and that they are inclined at angles  $\phi_i, \phi_j$ , respectively, as shown in [Fig. 1](#). It follows that the coordinates of the tips  $A, B$  of crack  $j$  are defined globally by

$$\zeta_A = \zeta_j + a_j e^{i\phi_j}, \quad \zeta_B = \zeta_j - a_j e^{i\phi_j} \quad (29)$$

and in the coordinate system  $(x', y')$  local to crack  $i$ ,

$$\zeta_A = (\zeta_j - \zeta_i + a_j e^{i\phi_j}) e^{-i\phi_i}, \quad \zeta_B = (\zeta_j - \zeta_i - a_j e^{i\phi_j}) e^{-i\phi_i}. \quad (30)$$

The force transmitted across the surface of crack  $j$  is then obtained *in coordinates local to crack i* by substituting (30) and their conjugates into (26)–(28) and hence into (24). However, to extract the corresponding contributions to the nodal forces  $P_j, Q_j$ , we need to perform another rotation (through the angle  $\phi_j - \phi_i$ ) into the coordinate system local to crack  $j$ , obtaining

$$Q + iP = -i(\psi_A - \psi_B) e^{-(\phi_j - \phi_i)}. \quad (31)$$

The off-diagonal influence coefficients ( $i \neq j$ ) of Eq. (22) are then defined by the relations

$$A_{ji} + iB_{ij} = -\frac{8\mu}{\pi(\kappa+1)} (\psi_A^{(v)} - \psi_B^{(v)}) e^{-(\phi_j - \phi_i)}, \quad (32)$$

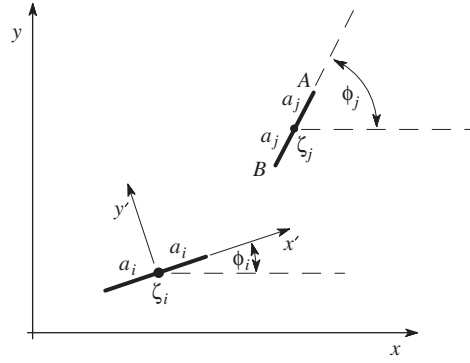


Fig. 1. Coordinate systems defining the relative position and orientation of cracks  $i$  and  $j$ .

$$B_{ji} + iC_{ji} = -\frac{8\mu}{\pi(\kappa+1)}(\psi_A^{(w)} - \psi_B^{(w)})e^{-(\phi_j - \phi_i)}, \tag{33}$$

where the arguments of these functions are defined by (30).

The diagonal components ( $i=j$ ) comprise the self-influence coefficients, which were already determined in Eq. (21), giving

$$A_{jj} = C_{jj} = \frac{16\mu}{\pi(\kappa+1)}, \quad B_{jj} = 0 \quad \text{no sum.} \tag{34}$$

In evaluating the complex expressions (27), (28), care must be taken to ensure that the square roots are evaluated along a consistent branch. This is best achieved by writing

$$\sqrt{\zeta^2 - a_i^2} = \sqrt{\zeta - a_i} \sqrt{\zeta + a_i} \tag{35}$$

and defining the square roots such that

$$\sqrt{s+it} = r^{1/2} \exp(i\varphi/2), \tag{36}$$

where

$$r^2 = s^2 + t^2 \quad \text{and} \quad \varphi = \text{sgn}(t) \arccos(t/r) \tag{37}$$

the inverse cosine being defined in the principal range  $0 < \varphi < \pi$ .

Also, if the distance

$$r_{ij} = \sqrt{(x_j - x_i)^2 + (y_j - y_i)^2} \tag{38}$$

between the crack centres is large compared with the crack lengths ( $r_{ij} \gg a_i a_j$ ), round-off errors may become significant. However, in this limit, the influence coefficients are very small and can reasonably be replaced by the values based on the traction at the crack mid-point, which are

$$\begin{aligned} A_{ji} &= -\frac{8\mu a_j a_i \cos(4\alpha_{ij} - 2\phi_i - 2\phi_j)}{\pi(\kappa+1)r_{ij}^2}, \\ B_{ji} &= -\frac{8\mu a_j a_i [\sin(4\alpha_{ij} - 2\phi_i - 2\phi_j) - \sin(2(\alpha_{ij} - \phi_j))]}{\pi(\kappa+1)r_{ij}^2}, \\ C_{ji} &= -\frac{8\mu a_j a_i [\cos(2(\alpha_{ij} - \phi_i)) + \cos(2(\alpha_{ij} - \phi_j)) - \cos(4\alpha_{ij} - 2\phi_i - 2\phi_j)]}{\pi(\kappa+1)r_{ij}^2}, \end{aligned} \tag{39}$$

$i \neq j$ , where  $\alpha_{ij} = \arg(\zeta_j - \zeta_i)$ .

The approximation involved in replacing the actual tractions at a given crack by their averages has the unfortunate effect of making the stiffness matrix for the discrete system slightly unsymmetrical. The asymmetry is significant only for quite closely spaced cracks. For example, if the matrix associated with a single crack pair is partitioned into symmetric and skew-symmetric parts, the norm of the skew-symmetric part is only of the order of one percent of that of the symmetric part, even when  $r_{ij}$  is comparable with the crack lengths  $a_i, a_j$ . In order to define a self-consistent structural system, we therefore chose to approximate the stiffness matrix by its symmetric part.

#### 4. Implications for media with microcracks

To apply these results to a microcracked plate, we first need to identify the specific characteristics of the crack population. In particular, we need to identify  $N$  sets of parameters  $\{x_i, y_i, a_i, \phi_i\}$  defining the coordinates of the centre of each crack, and its half-length and orientation. Typically, these quantities will only be known or estimated from statistical descriptions of the microstructure. For example, we may start from an assumed probability function  $P(x, y, a, \phi)$  and use a random number generator to develop one or more realizations of the actual crack locations, lengths and orientations. In many cases, the probability will be spatially uniform (independent of  $x, y$ ) and if the structure is on average isotropic, it will also be independent of  $\theta$ . However, we remark that clustered or indeed quasi-fractal crack distributions might be appropriate in many cases (Carpinteri and Spagnoli, 2004). Once a specific realization has been identified, the matrices  $\mathbf{A}, \mathbf{B}, \mathbf{C}$  can be determined following the procedure of Section 3.1.

The external loading is completely characterized by the imposed far-field stress components which we denote by  $S_{xx}(t), S_{yy}(t), S_{xy}(t)$ , and which can be fairly general functions of time  $t$ . To determine the functions  $Q_j^w, P_j^w$  of Eqs. (22), (23), we must first transform the stress field into the coordinate system local to crack  $j$ , obtaining

$$\sigma_{xy}^{(j)} = S_{xy} \cos(2\phi_j) - \frac{(S_{xx} - S_{yy}) \sin(2\phi_j)}{2},$$

$$\sigma_{yy}^{(j)} = \frac{(S_{xx} + S_{yy})}{2} - \frac{(S_{xx} - S_{yy}) \cos(2\phi_j)}{2} - S_{xy} \sin(2\phi_j).$$

Eqs. (2), (8) then give

$$Q_j^w = -2S_{xy} a_j \cos(2\phi_j) + (S_{xx} - S_{yy}) a_j \sin(2\phi_j),$$

$$P_j^w = -(S_{xx} + S_{yy}) a_j + (S_{xx} - S_{yy}) a_j \cos(2\phi_j) + 2S_{xy} a_j \sin(2\phi_j). \quad (40)$$

##### 4.1. Evolution of the system

The response of the cracked body to arbitrary time-varying far-field stress can now be determined by applying the evolution rules (15)–(20) to (22), (23). Various algorithms exist for this purpose. A fairly straightforward approach is to assume tentatively that the state of the  $N$  cracks at time  $t$  applies unchanged during a time increment  $\Delta t$ , in which case the Eqs. (15)–(20) permit the new values of  $v_j, w_j, Q_j, P_j$  to be calculated. These values are then checked against the governing inequalities and changes are made in the state assumptions until a consistent solution is obtained. A detailed description of an algorithm of this type is given by Ahn and Barber (2008).

Alternatively, a mathematically exact, non-iterative solution can be generated by recognizing that the system remains linear during any period for which the set of crack states remains unchanged. We can therefore solve for the point in the load cycle at which the next such state change occurs and make an appropriate ‘pivot’ at this point to a new state set. Klarbring and Björkman (1988) used this strategy to reduce the problem to a generalized linear complementarity problem (LCP). A more elegant algorithm is briefly described by Funk and Pfeiffer (2003) and has been implemented and explained in more detail by Bertocchi (2008).

##### 4.2. Effect of initial conditions

Frictional problems are history-dependent (Kachanov, 1982; Dundurs and Comninou, 1983, Lehner and Kachanov, 1995). For example, a single crack under constant compressive and shear loading can adopt a range of slip displacements  $v_j$  whilst still satisfying the stick inequalities (19). The actual state realized depends on the initial condition and the subsequent history of the loading. The ‘system memory’ can be characterized by the set of slip displacements at nodes that are instantaneously in a state of stick, so if there is any instant in the loading cycle at which all cracks are slipping or are open, dependence on previous stages of the loading is lost.

Suppose that the cracked body is subjected to loading that is periodic in time—for example

$$\mathbf{S} = \mathbf{S}_0 + \lambda \mathbf{S}_1 \exp(i\omega t), \quad (41)$$

where  $\mathbf{S} = \{S_{xx}, S_{xy}, S_{yy}\}$ , and we wish to determine the energy dissipated per cycle in frictional slip. We anticipate that the system will eventually converge on a steady state, but we have no guarantee that this state is unique—it could depend on the initial conditions. Comparatively few general results have been proved for such systems, but a frictional version of Melan’s theorem can be established (Klarbring et al., 2007) if and only if the system is uncoupled, which in the present notation corresponds to the case where the coupling matrix  $\mathbf{B} = \mathbf{0}$ . In this case, the theorem states that the system will shake down—i.e. reach a steady state in which there is no further frictional slip and hence no dissipation—if there exists any set of slip displacements sufficient to ensure that conditions at each node remain within the appropriate friction cone at all times. In other words, the system will shake down ‘if it can’. The resulting state is not generally unique, since there may exist several

such sets of slip displacements, but the time-varying terms in the resulting stress field (and therefore, for example, in the stress intensity factors) are unique.

Ahn et al. (2008) established a methodology for determining bounds  $\lambda_1, \lambda_2$  on the scalar load factor  $\lambda$  in Eq. (41) such that shakedown occurs for all initial conditions if  $\lambda < \lambda_1$  and never occurs for  $\lambda > \lambda_2$ . Melan's theorem is equivalent to the statement that  $\lambda_1 = \lambda_2$ , but for any coupled frictional elastic system ( $\mathbf{B} \neq \mathbf{0}$ ), there always exists a range  $\lambda_1 < \lambda < \lambda_2$  in which the system may either shake down or not, depending on the initial conditions.

It is tempting to speculate that the frictional Melan's theorem is a special case of a more general theorem to the effect that the time-varying terms in the steady state (and hence the dissipation and the effective internal damping) are independent of initial conditions if and only if  $\mathbf{B} = \mathbf{0}$ , but so far no-one has provided a proof of this result. It is however easy enough to generate specific loading scenarios for coupled systems (e.g. values of  $\lambda > \lambda_2$ ), where the dissipation does depend on initial conditions.

Notice that for the discrete frictional system equivalent to the microcracked body, only the off-diagonal components of  $\mathbf{B}$  can be non-zero, and these values reflect the interaction between cracks. We might speculate that dependence on initial conditions should correlate with the norm of the matrix  $\mathbf{B}$ , or more probably with appropriate sub-norms corresponding to the most highly interacting cracks. This in turn will depend on the crack density and on patterns of crack clustering, which might be characterizable in terms of fractals (Carpinteri and Spagnoli, 2004).

For a sufficiently large crack population, the distribution of relative crack orientations and clusters should be statistically stable, but the degree of interaction will correlate with the ratio between crack length and inter-crack spacing. We might therefore define a tentative measure of the degree of crack interaction as

$$\mathcal{I} = \frac{1}{N} \sum_{j=1}^N \frac{a_j}{r_{ji}^{\min}}, \quad (42)$$

where  $r_{ji}^{\min}$  is the distance from the centre of crack  $j$  to that of its nearest neighbour.

## 5. Some numerical results

To illustrate these arguments and assess the level of crack interaction  $\mathcal{I}$  at which coupling effects become significant, we used Ahn et al.'s (2008) algorithm to analyse the transient behaviour of a system of 10 cracks whose centres were randomly distributed in a unit square and whose sizes and orientations were randomly assigned. The mean value of the crack semi-length was set at

$$\bar{a} = \frac{1}{N} \sum_{i=1}^N a_i = 0.1. \quad (43)$$

A rather modest number of cracks was used at this stage of the investigation, because (i) we wish to explore the effect of initial conditions and with 10 cracks, this already represents a space of 10 dimensions and (ii) the use of Ahn et al.'s (2008) algorithm to determine  $\lambda_1, \lambda_2$  becomes combinatorially more complex as the number of cracks increases.

A particular realization is shown in Fig. 2, corresponding to a value  $\mathcal{I} = 0.49$ . The system was subjected to loading of the form (41) with

$$\mathbf{S}_0 = p_0\{-1, 0, -1\} \quad \text{and} \quad \mathbf{S}_1 = p_0\{0, 1, 0\}.$$

In other words, the mean stress state is hydrostatic compression of magnitude  $p_0$  and the oscillating stress is pure shear of magnitude  $\lambda p_0$ .

A sufficient number of cycles were analysed for the behaviour to reach a steady state. Fig. 3(a) shows the normalized steady-state energy dissipated in friction per cycle

$$W^* \equiv \frac{W\mu}{(\kappa+1)p_0^2\bar{a}^2}$$

as a function of the scalar load factor  $\lambda$ . Notice that these results hold for all values of  $p_0$ , since the contact problem falls under the category of *receding contact* defined by Dundurs and Stippes (1970) and hence is linear in  $p_0$ , despite the presence of inequalities in the problem formulation. By contrast, the factor  $\bar{a}^2$  is included in order to make  $W^*$  dimensionless, but changes in  $\bar{a}$  will change the interaction coefficient  $\mathcal{I}$  and hence will generally change the dissipation.

Numerous different initial conditions (values of  $v_i(0)$ ) were chosen for each case and the minimum and maximum values of dissipation obtained are represented by  $\triangle$  and  $\circ$ , respectively. The values  $\lambda_1 = 0.5628, \lambda_2 = 0.5878$  were determined from Ahn et al.'s (2008) algorithm and define, respectively, the values below which shakedown (zero dissipation) occurs for *all* initial conditions, and above which shakedown cannot occur for *any* initial condition. This behaviour is clear from the zoom in Fig. 3(c) which shows that the minimum dissipation is zero in  $\lambda_1 < \lambda < \lambda_2$ , whereas the maximum is non-zero.

The results show a modest dependence of dissipation on initial conditions at values not too far above  $\lambda_2$ , but this dependence becomes a negligible proportion of the total dissipation at higher values, as shown in Fig. 3(b). In fact, completely unique steady state dissipation was obtained for  $\lambda \geq 1.2$ . This could simply be the result of the necessarily limited range of initial conditions explored, but there are theoretical reasons to believe that there does exist some upper bound to  $\lambda$  above which the cyclic response is unique. We recall that the history of the system resides in the instantaneous slip displacements at

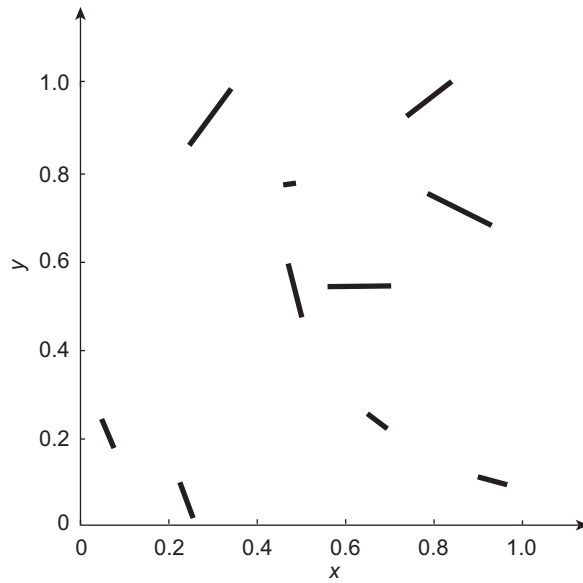


Fig. 2. A random distribution of microcracks.

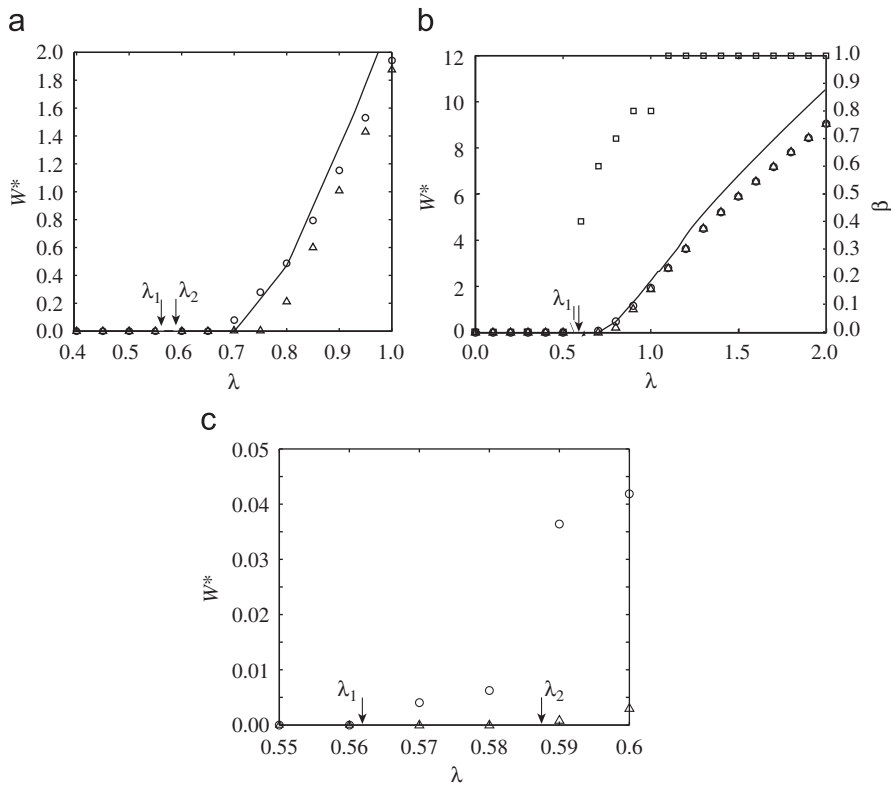


Fig. 3. Dissipation as a function of the loading factor  $\lambda$  in Eq. (41). The solid line in (a) and (b) shows the dissipation if interaction is neglected and the symbols  $\Delta$ ,  $\circ$  show the minimum and maximum dissipation, respectively, depending on initial conditions. In (b), the symbol  $\square$  represents the proportion  $\beta$  of cracks that slip and/or open at some time during the steady state.

the stuck nodes (cracks). If  $\lambda$  is sufficiently large to ensure that all cracks either slip or open at some point during the cycle, this ‘history’ must be repeatedly exchanged from node to node and there is every reason to expect that this exchange process will lead at least asymptotically to a loss of information and hence to a final unique steady state. We therefore plot in Fig. 3(b) the

proportion  $\beta$  of cracks that slip and/or open at least once during the steady state and confirm that all the cracks meet this condition for  $\lambda > 1.2$ .

The fact that dissipation is unique at sufficiently large  $\lambda$  suggests that the results in this range might be dominated by the ‘uncoupled’ response—i.e. the diagonal terms in the matrices  $\mathbf{A}, \mathbf{C}$ . To test this hypothesis, we calculated the dissipation due only to the diagonal elements, which is equivalent to the simplifying assumption (‘zeroth-order interaction’) that each crack acts independently under the influence of the applied far-field stress. This can be determined by running the transient algorithm, but a quicker calculation, better suited to large crack populations, is to analyse the behaviour of a generically loaded crack  $j$  and then perform a suitable summation over  $j \in (1, N)$ . The analysis is given in the Appendix and the results are summarized in Eq. (44), with  $k=C_{jj}$  given by (34). These results are plotted as the solid line in Fig. 3(b). For the cases studied, the interaction terms lead to somewhat less dissipation than in the uncoupled case and this difference increases with increasing load amplitude. Thus, the uncoupled solution is unlikely to give accurate estimates for hysteretic damping for any but the most sparse of crack distributions.

5.1. Effect of the interaction coefficient

The results in Fig. 3 show that the first-order interaction terms decrease the dissipation relative to the uncoupled solution, but other realizations of the same crack statistics showed that this was not a universal result. In fact, with only 10 cracks, any trend in the effect of the interaction terms was swamped by statistical scatter. Real materials will typically contain much

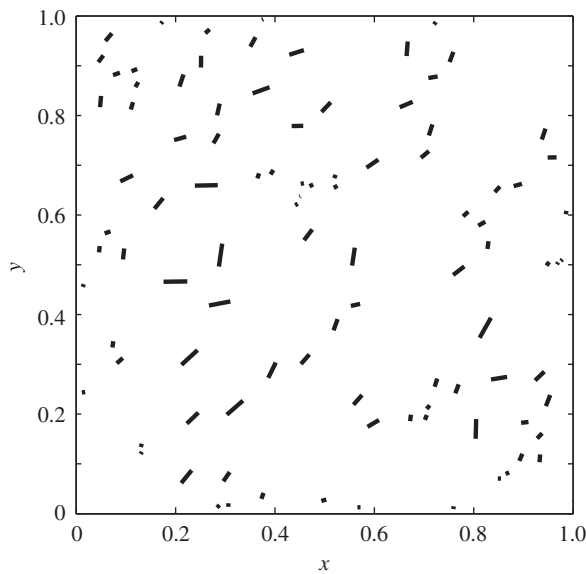


Fig. 4. A representative crack distribution, corresponding to  $\mathcal{I} = 0.3826$ .

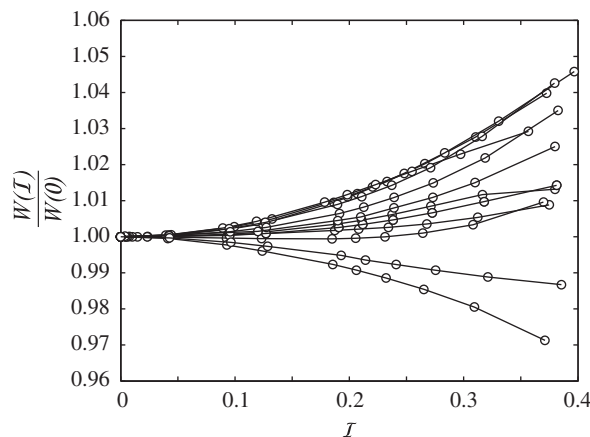


Fig. 5. Effect of the interaction coefficient  $\mathcal{I}$  on the energy dissipated in friction for  $\lambda = 5$ . The various curves represent different realizations of the same crack statistics.

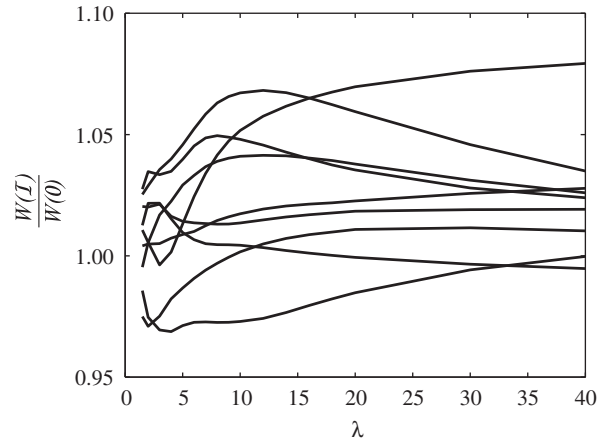


Fig. 6. Effect of the load factor  $\lambda$  on the energy dissipated in friction for  $\mathcal{I} = 0.38$  and several different realizations of the same crack statistics.

larger populations of microcracks and this will tend to moderate the differences in dissipation between different realizations. We therefore explored the effect of the interaction coefficient  $\mathcal{I}$  of Eq. (42), using a set of 100 cracks. A particular realization is shown in Fig. 4.

The crack lengths were chosen to give a mean value  $\bar{a} = 0.01$  within a  $1 \times 1$  square, since this preserves values of  $\mathcal{I}$  that are comparable with those of Fig. 2. Different values of  $\mathcal{I}$  were then achieved by scaling the coordinates defining the locations of the cracks (and hence the dimensions of the square), so as to reduce or increase the inter-crack lengths  $r_{ij}$ .

Fig. 5 shows the dissipation as a function of  $\mathcal{I}$  for  $\lambda = 5$  and various realizations of the same crack statistics, normalized by the ‘uncoupled’ dissipation predicted by Eq. (44).

There is still significant statistical variation between the various realizations, but in most cases the dissipation is *increased* by crack interaction and the proportional change is found to be approximately proportional to  $\mathcal{I}^2$ .

Fig. 6 shows the effect of the scalar load factor  $\lambda$  on the normalized dissipation for various realizations of the same crack statistics with  $\mathcal{I} = 0.38$ . The results show quite complex and often non-monotonic dependence on  $\lambda$ . For each realization, the dissipation tends to a constant proportion of the uncoupled value at large  $\lambda$  and this ratio is usually (but not always) somewhat larger than unity. In this range, most cracks will be open for about half the loading cycle. Overall, we conclude that at this level of crack interaction, the uncoupled analysis provides a reasonable first approximation to the frictional dissipation.

## 6. Conclusions

A major objective of this paper is to exhibit the relation between the first order Kachanov model of the interaction between  $N$  interacting plane cracks, and a discrete  $N$ -node frictional system, such as that generated by finite element analysis of a two-dimensional frictional contact problem. Since algorithms for such discrete systems are well established, this represents an efficient way of investigating the effect of crack interaction when frictional sliding is present. In particular, we demonstrate that the energy dissipation per cycle (internal damping) depends on initial conditions if the system is dominated by a compressive mean stress, but becomes unique if the oscillating loading is sufficiently large to ensure that all cracks slip at least once during each cycle.

The limiting value of dissipation when crack interaction is negligible can be obtained by a simple summation of closed form expressions. When interaction effects are included, dissipation varies significantly between different realizations of the same crack statistics and these differences increase quadratically with the mean reciprocal of the intercrack spacing for a given set of crack orientations. The ratio between the coupled and uncoupled dissipation tends to a constant value when the oscillating stress is large compared with the compressive mean stress.

## Appendix A. Dissipation in the uncoupled solution

We consider a frictional system comprising one contact node (crack) subject to the loading

$$P(t) = P_0 + P_1 g(t), \quad Q(t) = Q_1 g(t),$$

where  $P, Q$  are the normal (compressive) and tangential external forces and  $g(t)$  is a periodic (e.g. sinusoidal) function of time  $t$  with maximum and minimum values  $\pm 1$ . The coefficient of friction at the interface is  $f$  and tangential motion (slip) is opposed by a spring of stiffness  $k$ , which in the case of crack  $j$  is given by  $C_{jj}$  of Eq. (34). We wish to determine the amount of energy dissipated in friction during one cycle. We restrict  $P_0, P_1, Q_1$  to the ranges

$$P_0 > 0, \quad P_1 > 0, \quad Q_1 > 0.$$

Notice that there is no loss of generality in taking  $Q_1, P_1 > 0$ , since we can always choose the coordinate directions and the phase of the periodic load to ensure that these conditions are satisfied.

If  $P_0 > P_1$  there will be no separation and, if slip occurs, the maximum slip displacement  $v_{\max}$  will occur at  $g(t)=1$  and the maximum negative value at  $g(t)=-1$ . Once slip occurs, the system 'memory' is erased, so after the first slip period, the system will achieve a periodic steady state.

We start from the state at  $g(t)=1$ . This must be reached as a result of forward slip  $\dot{v} > 0$  and hence the instantaneous friction force acts in the negative  $x$ -direction and is of magnitude

$$fP = f(P_0 + P_1).$$

It follows from equilibrium considerations that

$$Q_1 - f(P_0 + P_1) - kv_{\max} = 0 \quad \text{or} \quad kv_{\max} = Q_1 - f(P_0 + P_1).$$

The time derivative  $g'(t)$  now changes direction and the system sticks until the reaction is sufficiently large for slip to start in the opposite direction. The force in the spring is unchanged, so at the beginning of backward slip, we have

$$Q_1 g + f(P_0 + P_1 g) - kv_{\max} = 0.$$

Eliminating  $v_{\max}$ , we have

$$Q_1 g + f(P_0 + P_1 g) - Q_1 + f(P_0 + P_1) = 0 \quad \text{or} \quad g_1 = \frac{(Q_1 - 2fP_0 - fP_1)}{(Q_1 + fP_1)},$$

where we denote by  $g_1$  the value of  $g(t)$  at which backward slip commences. We notice that this result is meaningful if and only if  $-1 < g_1 < 1$ . With the above sign conventions, we have  $Q_1 + fP_1 > 0$  and hence the condition  $g_1 > -1$  gives

$$Q_1 - 2fP_0 - fP_1 > -Q_1 - fP_1 \quad \text{or} \quad Q_1 > fP_0.$$

If instead  $Q_1 < fP_0$ , slip will never start and the system will shake down. The other inequality,  $g_1 < 1$  can be shown to be satisfied identically for  $P_0 > 0$ .

During backward slip, the friction force is

$$F = f(P_0 + P_1 g(t))$$

and the slip displacement  $v$  is given by

$$Q_1 g(t) + f(P_0 + P_1 g(t)) - kv = 0 \quad \text{or} \quad kv = (Q_1 + fP_1)g(t) + fP_0.$$

Differentiating with respect to time, we then have

$$k\dot{v} = (Q_1 + fP_1)g'(t)$$

and the rate of power dissipation due to slip is

$$\dot{W} = -F\dot{v} = -\frac{f(P_0 + P_1 g(t))(Q_1 + fP_1)g'(t)}{k}.$$

The total energy dissipated during the half-cycle is therefore

$$W_1 = \int \dot{W} dt = -\frac{1}{k} \int_{g_1}^{-1} f(P_0 + P_1 g)(Q_1 + fP_1) dg = \frac{f(Q_1 + fP_1)}{2k} [2P_0 g_1 + P_1 g_1^2 + 2P_0 - P_1].$$

Substituting for  $g_1$  and simplifying, we obtain

$$W_1 = \frac{2f(Q_1 - fP_0)(P_0 Q_1 - fP_1^2)}{k(Q_1 + fP_1)}.$$

The system will stick when  $g = -1$  and an exactly parallel analysis of the subsequent forward slip phase leads to the expression

$$W_2 = \frac{2f(Q_1 - fP_0)(P_0 Q_1 - fP_1^2)}{k(Q_1 - fP_1)}$$

for the energy dissipation during the second half cycle. The total energy dissipated per cycle is therefore

$$W = W_1 + W_2 = \frac{2f(Q_1 - fP_0)(P_0 Q_1 - fP_1^2)}{k(Q_1 + fP_1)} + \frac{2f(Q_1 - fP_0)(P_0 Q_1 - fP_1^2)}{k(Q_1 - fP_1)} = \frac{4fQ_1(Q_1 - fP_0)(P_0 Q_1 - fP_1^2)}{k(Q_1^2 - f^2 P_1^2)}.$$

This result is valid as long as the no-separation inequality  $P_0 > P_1$  is satisfied and  $Q_1 > fP_0$ .

If instead  $P_1 > P_0$ , separation will occur when

$$P_0 + P_1 g(t) < 0 \quad \text{or} \quad g(t) < g_0 = -\frac{P_0}{P_1}.$$

The easiest place to start this cycle is at  $g(t) = -1$ , where the system must be in a state of separation which will persist until  $g = g_0$ . Contact now starts with both normal and tangential contact reactions being zero. If  $Q_1 < fP_1$ , no slip will occur and the energy dissipation will be zero.

If  $Q_1 > fP_1$ , forward slip  $\dot{g} > 0$  will occur and will persist until  $g = 1$ . The work done during this phase is defined by

$$W_2 = \frac{f(Q_1 - fP_1)(1 - g_0)}{2k} [2P_0 + P_1(1 + g_0)] = \frac{f(Q_1 - fP_1)(P_1 + P_0)^2}{2kP_1}$$

after substituting for  $g_0$  and simplifying.

During the next phase  $\dot{g} < 0$ , slip starts at

$$g_1 = \frac{(Q_1 - 2fP_0 - fP_1)}{(Q_1 + fP_1)}$$

as in the case with no separation, but separation starts at  $g_0$ , so the integral must be performed between these limits. We obtain

$$W_1 = \frac{1}{k} \int_{g_0}^{g_1} f(P_0 + P_1g)(Q_1 + fP_1) dg = \frac{f(Q_1 - fP_1)^2(P_0 + P_1)^2}{2kP_1(Q_1 + fP_1)}$$

after substituting for  $g_1, g_0$ .

The total energy dissipation per cycle in the case of separation is then

$$W = W_1 + W_2 = \frac{fQ_1(Q_1 - fP_1)(P_0 + P_1)^2}{kP_1(Q_1 + fP_1)}.$$

These results can be extended to the range  $P_1 < 0$  and/or  $Q_1 < 0$  by replacing these parameters by their absolute values. The dissipation per cycle can therefore be summarized as

$$\begin{aligned} W &= 0, \quad |P_1| < P_0, \quad |Q_1| < fP_0 \\ &= \frac{4f|Q_1|(|Q_1| - fP_0)(P_0|Q_1| - fP_1^2)}{k(Q_1^2 - f^2P_1^2)}, \quad |P_1| < P_0, \quad |Q_1| > fP_0 \\ &= 0, \quad |P_1| > P_0, \quad |Q_1| < f|P_1| \\ &= \frac{f|Q_1|(|Q_1| - f|P_1|)(P_0 + |P_1|)^2}{k|P_1|(|Q_1| + f|P_1|)}, \quad |P_1| > P_0, \quad |Q_1| > f|P_1|. \end{aligned} \quad (44)$$

## References

- Ahn, Y.J., Bertocchi, E., Barber, J.R., 2008. Shakedown of coupled two-dimensional discrete frictional systems. *J. Mech. Phys. Solids* 56, 3433–3440.
- Ahn, Y.J., Barber, J.R., 2008. Response of frictional receding contact problems to cyclic loading. *Int. J. Mech. Sci.* 50, 1519–1525.
- Barber, J.R., 2010. *Elasticity*, third ed. Springer, Dordrecht (Section 13.3).
- Basista, M., Gross, D., 2000. A note on crack interaction under compression. *Int. J. Fract.* 102, 67–72.
- Bertocchi, E. Selected topics on the plane elastic contact with friction. Ph.D. Dissertation, Dipartimento di Ingegneria Meccanica e Civile, Università degli Studi di Modena e Reggio Emilia Via Vignolesse 905, Modena, Italy.
- Bower, A.F., 2010. *Applied Mechanics of Solids*. CRC Press, Boca Raton (Section 5.3.6).
- Carpinteri, A., Spagnoli, A., 2004. A fractal analysis of size effect on fatigue crack growth. *Int. J. Fatigue* 26, 125–133.
- Dundurs, J., Comninou, M., 1983. An educational elasticity problem with friction—Part III: General load paths. *ASME J. Appl. Mech.* 50, 77–84.
- Dundurs, J., Stippes, M., 1970. Role of elastic constants in certain contact problems. *ASME J. Appl. Mech.* 37, 965–970.
- England, A.H., 1971. *Complex Variable Methods in Elasticity*. John Wiley, London (Section 3.10).
- Fleck, N.A., 1991. Brittle fracture due to an array of microcracks. *Proc. R. Soc. A* 432, 55–76.
- Funk, K., Pfeiffer, F., 2003. A time-stepping algorithm for stiff mechanical systems with unilateral constraints. *Proc. Appl. Math. Mech.* 2, 228–229.
- Gambarotta, L., Lagomarsino, S., 1993. A microcrack damage model for brittle materials. *Int. J. Solids Struct.* 30, 177–198.
- Gavazza, S.D., Barnett, D.M., 1974. Elastic interaction between a screw dislocation and a spherical inclusion. *Int. J. Eng. Sci.* 12, 1025–1043.
- Gorbatikh, L., Lomov, S., Verpoest, I., 2007. On stress intensity factors of multiple cracks at small distances in 2-D problems. *Int. J. Fract.* 143, 377–384.
- Hills, D.A., Kelly, P.A., Dai, D.N., Korsunsky, A.M., 1996. *Solution of Crack Problems—The Distributed Dislocation Technique*. Kluwer, Dordrecht (Section 2.2).
- Kachanov, M., 1982. A microcrack model of rock inelasticity part 1: frictional sliding on microcracks. *Mech. Mater.* 1, 19–27.
- Kachanov, M., 1987. Elastic solids with many cracks: a simple method of analysis. *Int. J. Solids Struct.* 23, 23–43.
- Klarbring, A., Björkman, G., 1988. A mathematical programming approach to contact problems with friction and varying contact surface. *Comput. Struct.* 30, 1185–1198.
- Klarbring, A., Ciavarella, M., Barber, J.R., 2007. Shakedown in elastic contact problems with Coulomb friction. *Int. J. Solids Struct.* 44, 8355–8365.
- Lehner, F.K., Kachanov, M., 1995. On the stress–strain relations for cracked elastic materials in compression. In: Rossmannith, H.P. (Ed.), *Mechanics of Jointed and Faulted Rocks*. Balkema Press, Rotterdam, pp. 49–61.
- Li, Y.P., Tham, L.G., Wang, Y.H., Tsui, Y., 2003. A modified Kachanov method for analysis of solids with multiple cracks. *Eng. Fract. Mech.* 70, 1115–1129.
- Shao, J.F., Rudnicki, J.W., 2000. A microcrack-based continuous damage model for brittle geomaterials. *Mech. Mater.* 32, 607–619.